Journal of Electronics and Electrical Engineering
https://ojs.wiserpub.com/index.php/JEEE/

UNIVERSAL WISER PUBLISHER

Article

Analysis of Performance Improvement of Planar Antenna Arrays With Optimized Square Rings for Massive MIMO Applications

Jafar Ramadhan Mohammed* **and Abdulrazaq A. Khamees**

College of Electronic Engineering, Ninevah University, Mosul, Iraq
E-mail: jafar.mohammed@uoninevah.edu.iq

Received: 22 December 2023; **Revised:** 19 March 2024; **Accepted:** 22 March 2024

Abstract: The power pattern of the conventional fully optimized planar arrays can be properly reshaped according to the required user-defined constraints. However, the practical implementation of such fully optimized large planar arrays is complex and expensive. This paper introduces a new and efficient technique that is capable of providing better performance and almost the same power pattern shapes as that of the conventional fully optimized planar arrays by optimally adjusting the element amplitude and phase excitations of the outer-square rings instead of all elements' excitations. The proposed technique starts with a massive fully planar array then divides it into two contiguous sub-planar arrays which are both symmetric about the original array center. The elements excitation amplitudes or phases of the outer sub-planar array are only adjusted to form the desired power pattern shapes, while the amplitudes or phases of the central sub-planar array elements which have usually higher weights than the outer elements are made constants (i.e., they made ones for the case of amplitude-only control and zeros for the phase-only control). The results demonstrate the capability of the proposed planar array to form the required power patterns with far less number of the adjustable elements.

Keywords: two-dimensional rectangular planar antenna array, sidelobe level minimization, array pattern optimization, genetic algorithm

1. Introduction

Many of the modern radar and communication systems use two dimensional rectangular planar array configurations rather than a simple linear array configuration due to their flexibility and possibility to freely scanning their main beam directions in both azimuth and elevation planes. Generally, effective optimization algorithms such as practical swarm optimization (PSO) [1], Ant colony optimization algorithm [2], differential evolution (DE) algorithm [3],cross entropy (CE) method [4], convex optimization [5], fire-fly algorithm [6], and genetic optimization algorithm (GA) [7], can be used to optimally synthesis such planar arrays by finding the optimum values of the amplitudes and/or phases of the array elements that responsible for shaping the required power pattern. In the conventional fully adjustable planar arrays, the excitation amplitudes or phases of all the array elements are iteratively adjusted during the optimization process to achieve the required power pattern. Thus, such type of the arrays is usually difficult to implement in practice. They are also characterized as highly time consuming. Therefore, simpler and faster methods are highly advised. In [8], the authors suggested to adjust only the amplitude excitations of the array elements instead of both amplitude and phase excitations to simplify the design implementation of the array feeding network and reduce the number of the optimized variables. Other researchers suggested the use of the phase-only excitation method [9] to optimize the planar

DOI: https://doi.org/10.37256/jeee.3120244146

array elements. Recently, efficient methods for linear [10–14] and planar arrays [15–18] were suggested. In these methods only the side elements of the linear or planar arrays were adjusted during the optimization process to reach the required power pattern with desired nulls and sidelobe levels. In all of the methods that were presented in [10–18], the total number of the adjustable side-elements was chosen beforehand at a certain value. Thus, the optimized power patterns were found satisfactory only when there are sufficient numbers of the adjustable elements to fulfill the required constraints. Other method includes the use of the parasitic elements to obtain the optimized power pattern with simplified array configuration [19] or some advanced techniques [20,21].

In this paper, the authors present a simple automatic technique to partially optimize the planar arrays that are capable of providing almost the same desired power patterns as that of the conventional fully optimized planar arrays with far less number of the adjustable elements. The technique is based on the division of an initial planar array into two contiguous sub-planar arrays which are symmetric about the array center. The element excitations in terms of either amplitudes or phases of the outer sub-planar array are made adjustable and they are optimized to form the desired power pattern. In contrast to the previous methods [10–18], the number of the adjustable side-elements in the outer square rings is also made adaptive. This means that the optimization algorithm will optimally choose the required number of the adjustable outer-square rings. By this way, an excess in the number of the adjustable side-elements is avoided and only the exact number of the needed adjustable elements is identified. On the other hand, the elements' excitations of the central sub-planar array which they usually have higher amplitude weights are made constants. Thus, the convergence speed of the optimizer in the proposed technique is effectively shortened with compared to that of the conventional fully optimized planar arrays.

2. Proposed Method Principles

2.1 *Conventional Fully Rectangular Array*

Consider a symmetrical broadside planar array of isotropic elements with an even number of elements N × M as shown in Figure 1.

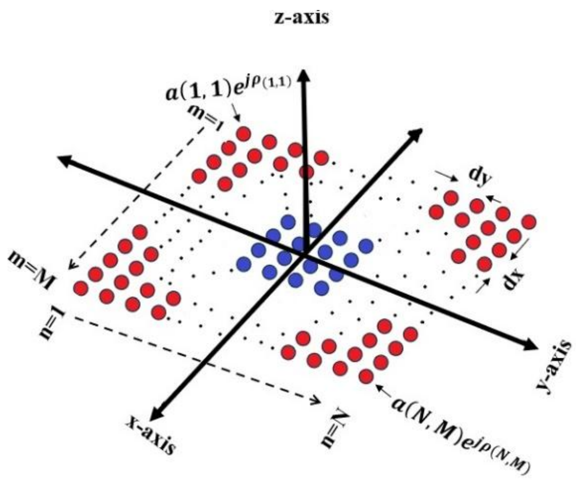

Figure 1. Planar Array Configuration.

The array factor expression of such planar array can be obtained by multiplying the array factors of the two linear arrays according to [22] as follows:

$$AF(\theta,\phi) = \sum_{n=1}^{N} \sum_{m=1}^{M} a_{nm} e^{j\rho_{nm}} e^{j[(m-1)\psi_x]} e^{j[(n-1)\psi_y]} \tag{1}$$

where a_{nm} and ρ_{nm} are the adjustable elements excitation amplitudes and phases respectively, $\psi_x = kd_x\sin\theta\cos\phi$, $\psi_y = kd_y\sin\theta\sin\phi$, d_x and $d_y$are the separation distances between the array elements along the *x*-axis and *y*-axis respectively, $k = 2\pi/\lambda$ and λ is the wavelength in free space. From (1), it can be seen that all the amplitudes and/or phases of the array elements are needed to be adjusted by the use of an optimization algorithm to obtain the required power pattern according to the particular shape constraints. Here in this paper, the amplitude-only control method (i.e., a_{nm} are optimized whereas ρ_{nm} are set to zeros) and the phase-only control method (i.e., ρ_{nm} are optimized and a_{nm} are set to ones) are adopted. Further, instead of adjusting all of the amplitudes, a_{nm}, or phases, ρ_{nm}, of the array elements, it is possible to efficiently adjust only part of the array elements while maintaining almost the same power pattern shapes as that of the fully optimized planar arrays.

2.2 *The Modified Planar Array With Optimized Perimeter Elements*

The fully planar array that was shown in Figure 1 is divided into two contiguous sub-planar arrays symmetrical about the array center. For simplicity, assume a square planar array with dimension $N = M$ and suppose that the number of the square rings in the outer sub-planar array is equal to L. Thus, the number of the adjustable elements that need to optimize their excitations in the outer sub-planar array is equal to $2\{2L(N-L)\}$. These adjustable elements are optimized to reach the required power pattern shapes according to the desired constraints. The amplitudes or phases of the remaining central sub-planar array elements are made to be ones or zeros respectively.

Thus, the array factor of (1) can be rewritten to express such division into central and outer sub-planar arrays:

$$AF(\theta,\phi) = \underbrace{\sum_{n=1}^{N-2L}\sum_{n=1}^{N-2L} e^{j\left[(n-1)(\psi_x+\psi_y)\right]}}_{\text{central sub-planar array}} + \underbrace{\sum_{n=N-2L+1}^{N}\sum_{n=N-2L+1}^{N} a_{nn} e^{j\rho_{nn}} e^{j\left[(n-1)(\psi_x+\psi_y)\right]}}_{\text{Louter square rings}} \tag{2}$$

As mentioned earlier, the values of a_{nn} and ρ_{nn} in the central sub-planar array are chosen to be 1 and 0 respectively. For amplitude–only control, the values of a_{nn} in the outer sub-planar array are only optimized, while for phase-only control the values of ρ_{nn} in the outer sub-planar array are optimized.

The optimization process was carried out by genetic algorithm to adjust the values of a_{nn} or ρ_{nn} such that the overall power pattern shape of the proposed planar array that expressed by (2) best matches the conventional array pattern in (1) and fulfils all the desired constraints. The optimization process should also find the best value of the number of the outer square rings, L. The flowcharts of the optimization processes of the conventional fully and the proposed partially optimized planar arrays can be summarized in Figure 2 below.

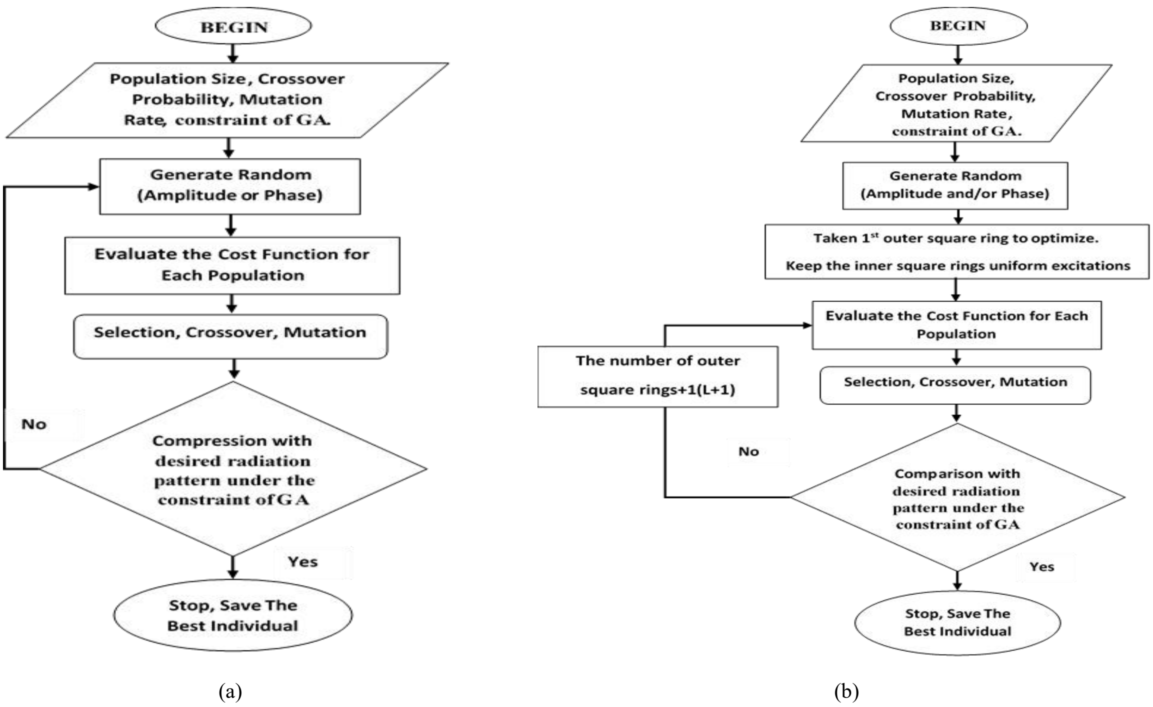

Figure 2. (a) Conventional Fully Optimized Array and (b) Proposed Partially Optimized Array.

The GA is used to optimize either the amplitudes, a_{nm}, or the phases, ρ_{nn}, of the adjustable outer sub-planar array elements. To find the best match between the power patterns of the conventional fully adjustable planar array elements and the proposed partially planar array elements, the following constraints are equally imposed on both radiation patterns. The constraints include the width and direction of the intended nulls, $\text{Null}_{(Depth,\ j)}$, peak *SLL*, and the width of the main beam as follows:

$$AF_{n\text{dB}}(\theta,\phi)=20\log_{10}\frac{AF(\theta,\phi)}{\max\left(AF(\theta,\phi)\right)} \tag{3}$$

where $AF_{n\text{dB}}(\theta,\phi)$ is the normalized array factor of (2) and in dB.

$$\left|AF_{n\text{dB}}(\theta_i,\phi_i)\right|\le 0\ \text{dB for}\ \left(-1/Nd_x\right)\le\theta_i\le\left(1/Nd_x\right)\ \text{and}\ \phi_i\ \text{constant} \tag{4}$$

$$\left|AF_{n\text{dB}}(\theta_i,\phi_i)\right|\le \text{SLL for}\ \left(-1/Nd_x\right)\ge\theta_i\ge\left(1/Nd_x\right)\ \text{and}\ \phi_i\ \text{constant} \tag{5}$$

$$\left|AF_{n\text{dB}}(\theta_j,\phi_j)\right|\le \text{Null}_{(Depth,\ j)}\ \text{for}\ j=1,2,\dots,\text{J} \tag{6}$$

where $1/N_{dx}$ is the angular position of the first null in the power pattern, θ_j is the null direction, and J is the total number of the nulls. The constraint in (4) represents the limits on the required main beam width, while the constraints in (5) and (6) represent the limits on the peak sidelobe level and the null directions respectively.

The cost function minimizes the difference between the desired power pattern according to the above constraints and the actual pattern that generated from the optimized elements.

3. Results of Simulation

To demonstrate the capability of the proposed technique, various illustrative scenarios have been simulated. The elements of the considered planar array with size N × N are divided into central and outer sub-planar arrays. The amplitudes or phases of the elements of the outer square rings which have more contribution to the array pattern reconfiguration are adjusted to form the optimized power pattern. The computations were performed for a large planar array of 20 × 20 elements with half-wavelength spacing in both x and y axes and the main beam directed toward the broadside. The main parameters of the GA are chosen as: population size of 50; selection is Tournament; crossover is two points; mutation rate is 0.2; mating pool is 10. The upper and lower values of the excitation amplitudes are bounded between 0 and 1, while the phases are bounded between −π/2 and π/2.

In the first example, we used amplitude-only control to optimize all the adjustable elements of the conventional planar array and compare its power pattern to that of the partially optimized planar array with a number of the adjustable outer square rings equal to L = 3, the required constraints are two nulls at directions 14.9°, 13.75° both with depth −55dB, and peak SLL = −18dB. Figure 3 and Figure 4 show the power patterns and the corresponding amplitude element excitations of the fully and partially optimized planar arrays. From these two figures, it observed that the power patterns of the fully and partially optimized arrays are both within the constraint limits but not exactly matched where there are slight differences in the sidelobe regions.

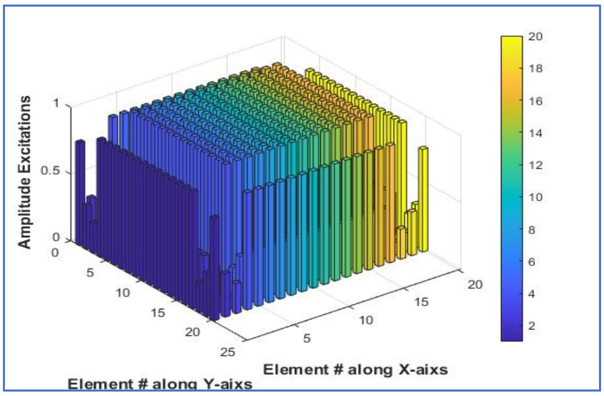

(a)

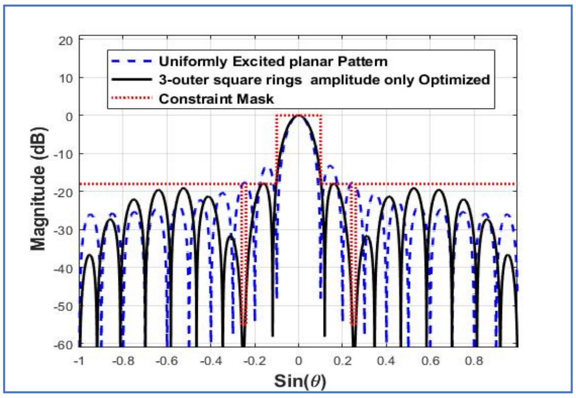

(b)

Figure 3. Fully optimized square array for 20 × 20 and amplitude-only control.

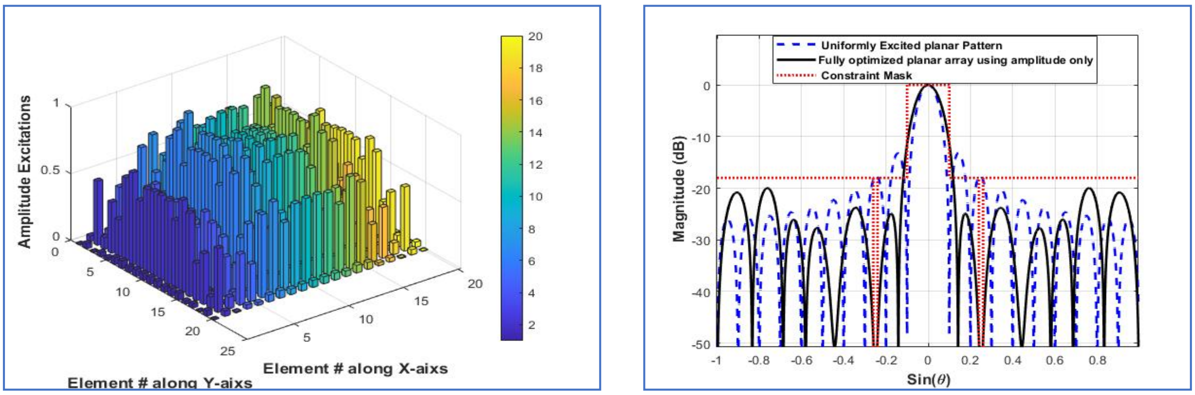

(a) (b)

Figure 4. Partially optimized square array for 20 × 20 and amplitude-only control.

In the second example, we used phase-only control to optimize both the fully and partially planar arrays. As in the previous example, we used only $L = 3$ outer square rings with the partially optimized array. Figure 5 and Figure 6 show the radiation patterns and the corresponding phase excitations of the fully and partially optimized planar arrays. From these two figures, it observed that the power patterns of the fully and partially optimized arrays are almost matched and both patterns met the constraint shapes. Moreover, the phase distributions of the fully and partially optimized arrays are approximately same especially for those elements that close to the array centre. These results, verify the superiority of the proposed partially optimized array with phase-only control.

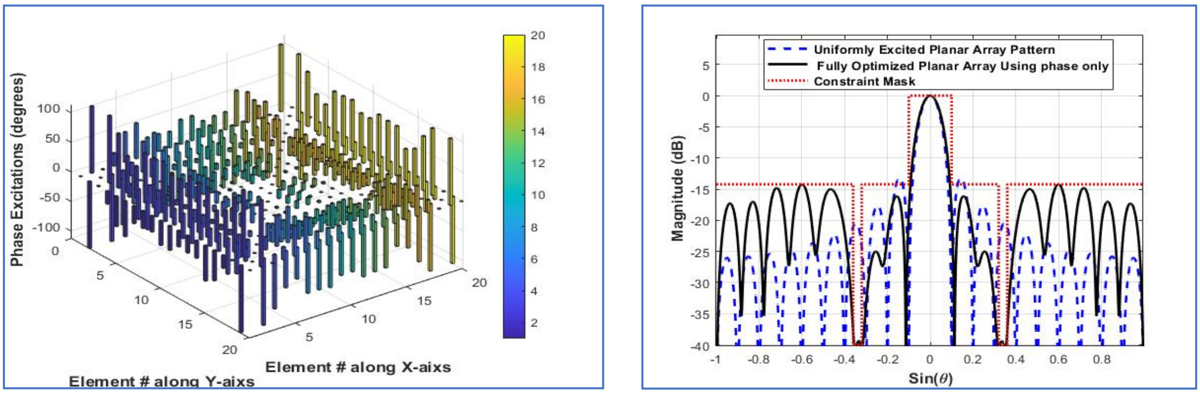

(a) (b)

Figure 5. Fully optimized square array for 20 × 20 and phase-only control.

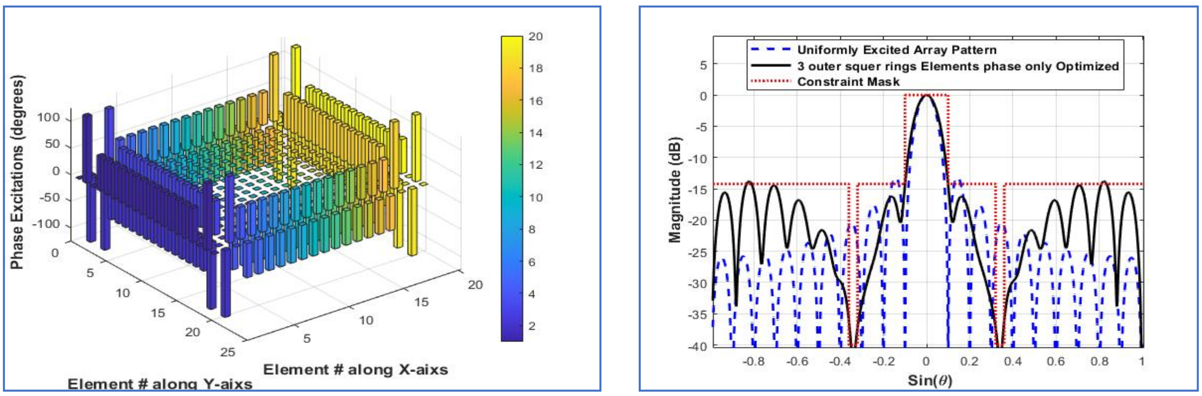

(a) (b)

Figure 6. Partially optimized square array for 20 × 20 and phase-only control.

In the next example, the performances of the proposed partially planar array in terms of directivity, complexity, taper efficiency, average sidelobes, and HPBW versus the number of the optimized elements in the outer square rings are investigated. Figure 7 shows the results of the proposed partially planar arrays under both amplitude-only and phase-only controls. From this figure, it observed that the proposed partially planar array with phase-only control gives the best performance under reasonable number of the outer square rings selection.

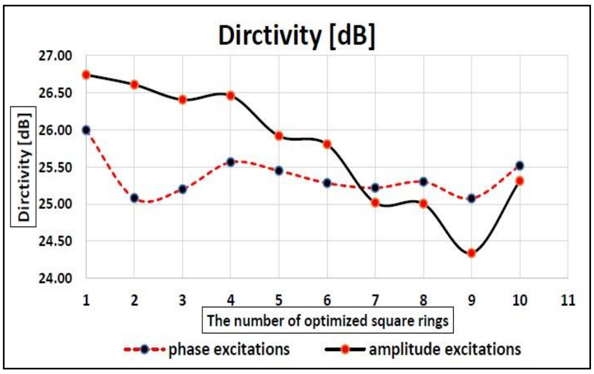

(a)

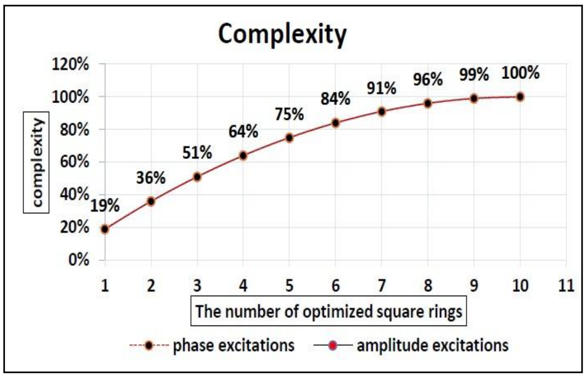

(b)

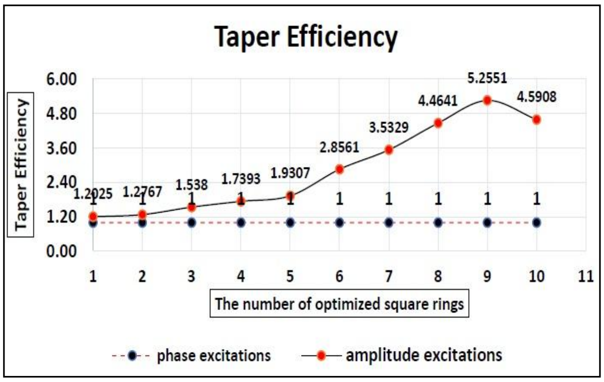

(c)

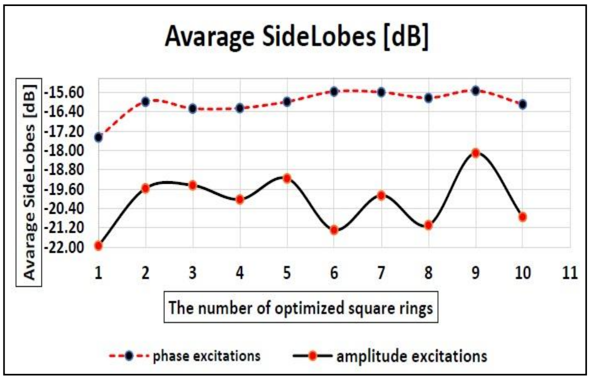

(d)

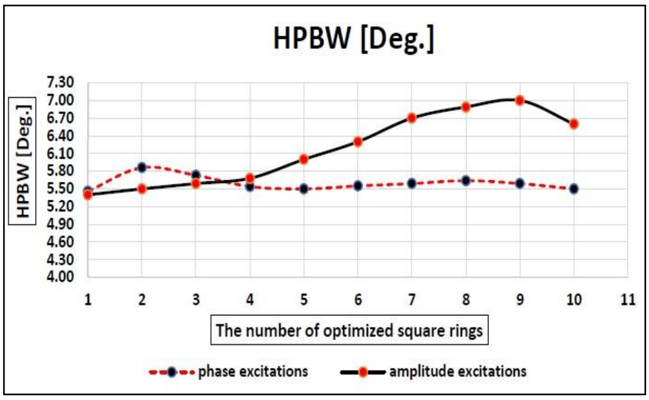

(e)

Figure 7. (a) The Directivity, (b) Complexity, (c) Taper Efficiency, (d) Average Side Lobes, and (e) HPBW of the partially optimized planar array versus the number of optimized square rings.

Finally, table 1 shows the numerical comparison between the tested methods. Here, the proposed partially planar array uses 3 outer square rings, i.e., the optimized outer elements were equal to 204 among total number of elements equal to 400.

Table 1. Performances of the Tested Methods for 20 × 20 array elements

Methods	Directivity [dB]	Average-SLL [dB]	Taper Efficiency	Peak SLL [dB]	FNBW [Deg.]	HPBW [Deg.]	Complexity Percentage
Uniformly Excited Array	27.07	−20	1	−13.23	11.46^0	5.05^0	0 %
Amplitude-Only Fully Optimized Array	25.31	−20.74	4.59	−28.92	17.7^0	6.6^0	100%
Amplitude-Only Partially Optimized Array with L = 3 rings	26.40	−19.44	1.53	−18.1	13.43^0	5.59^0	51%
Phase-Only Fully Optimized Array	25.47	−16.32	1	−14.23	12.95^0	5.54^0	100%
Phase-Only Partially Optimized Array with L = 3 rings	25.20	−16.26	1	−14.23	13.75^0	5.73^0	51%

4. Conclusion

It has been shown from the presented results that the same power pattern shapes with desired nulls and sidelobe levels can be equally obtained by both the fully and partially adjustable planar arrays. The key feature of the proposed partially adjustable approach lay on the number of the adjustable elements which is much lower than that of the conventional fully planar array. This gives the superiority of the proposed planar array especially when using phase-only control. The complexity in terms of the number of adjustable elements to the total number of the array elements is reduced from 100% for the conventional fully adjustable array to only 51% for the proposed array. Other advantages include the fastest convergence speed of the optimizer. Moreover, the directivity of the proposed partially adjustable array elements was found to be only slightly changed with compared to that of the conventional planar arrays.

Conflict of Interest

There is no conflict of interest for this study.

References

[1] Khodier, M.; Christodoulou, C. Linear array geometry synthesis with minimum sidelobe level and null control using particle swarm optimization. *IEEE Trans. Antennas Propag.* **2005**, *53*, 2674–2679, https://doi.org/10.1109/tap.2005.851762.

[2] Quevedo-Teruel, O.; Rajo-Iglesias, E. Ant Colony Optimization in Thinned Array Synthesis With Minimum Sidelobe Level. *IEEE Antennas Wirel. Propag. Lett.* **2006**, *5*, 349–352, https://doi.org/10.1109/lawp.2006.880693.

[3] Rocha-Alicano, C.; Covarrubias-Rosales, D.; Brizuela-Rodriguez, C.; Panduro-Mendoza, M. Differential evolution algorithm applied to sidelobe level reduction on a planar array. *AEU - Int. J. Electron. Commun.* **2007**, *61*, 286–290, https://doi.org/10.1016/j.aeue.2006.05.008.

[4] Abderrahmane, L.H.; Boussouar, B. New optimisation algorithm for planar antenna array synthesis. *AEU - Int. J. Electron. Commun.* **2012**, *66*, 752–757, https://doi.org/10.1016/j.aeue.2012.01.005.

[5] Zhang, Y.-X.; Jiao, Y.-C.; Zhang, L. Antenna Array Directivity Maximization With Sidelobe Level Constraints Using Convex Optimization. *IEEE Trans. Antennas Propag.* **2020**, *69*, 2041–2052, https://doi.org/10.1109/tap.2020.3026886.

[6] Yoshimoto, E.; Heckler, M.V. Optimization of planar antenna arrays using the firefly algorithm. *J. Microw. Optoelectron. Electromagn. Appl.* **2019**, *18*, 126–140, https://doi.org/10.1590/2179-10742019v18i11646.

[7] Haupt, R. Genetic algorithm design of antenna arrays. In 1996 IEEE Aerospace Applications Conference. Proceedings, Aspen, CO, USA, 10 February 1996, https://doi.org/10.1109/AERO.1996.495875.

[8] Guney, K.; Babayigit, B. Amplitude-only pattern nulling of linear antenna arrays with the use of a n immune algorithm. *Int. J. RF Microw. Comput. Eng.* **2008**, *18*, 397–409, https://doi.org/10.1002/mmce.20298.

[9] Abdulqader, A.J.; Mohammed, J.R.;Thaher, R.H. Phase-only nulling with limited number of controllable elements. *Prog. Electromagn. Res. C.* **2020**, *99*, 167–178, https://doi.org/10.2528/PIERC20010203.

[10] Mohammed, J. Optimal null steering method in uniformly excited equally spaced linear arrays by optimising two edge elements. *Electron. Lett.* **2017**, *53*, 835–837, https://doi.org/10.1049/el.2017.1405.

[11] Mohammed, J.R. Element Selection for Optimized Multiwide Nulls in Almost Uniformly Excited Arrays. *IEEE Antennas Wirel. Propag. Lett.* **2018**, *17*, 629–632, https://doi.org/10.1109/lawp.2018.2807371.

[12] Sayidmarie, K.H.; Mohammed, J.R. Performance of a wide angle and wide band nulling method for phased arrays. *Prog. Electromagn. Res. M.* **2013**, *33*, 239–249, https://doi.org/10.2528/pierm13100603.

[13] Mohammed, J.R. Thinning a subset of selected elements for null steering using binary genetic algorithm. *Prog. Electromagn. Res. M.* **2018**, *67*, 147–155, https://doi.org/10.2528/PIERM18021604.

[14] Mohammed, J.R. High-resolution Direction of Arrival Estimation Method Based on Sparse Arrays with Minimum Number of Elements. *J. Telecommun. Inf. Technol.* **2021**, *1*, 8–14, https://doi.org/10.26636/jtit.2021.143720.

[15] Mohammed, J.R. Simplified rectangular planar array with circular boundary for side lobe suppression. *Prog. Electromagn. Res. M.* **2020**, *97*, 57–68, https://doi.org/10.2528/pierm20062906.

[16] Mohammed, J.R. Obtaining wide steered nulls in linear array patterns by optimizing the locations of two edge elements. *AEU - Int. J. Electron. Commun.* **2019**, *101*, 145–151, https://doi.org/10.1016/j.aeue.2019.02.004.

[17] Mohammed, J.R.; Sayidmarie, K.H. Sidelobe Cancellation for Uniformly Excited Planar Array Antennas by Controlling the Side Elements. *IEEE Antennas Wirel. Propag. Lett.* **2014**, *13*, 987–990, https://doi.org/10.1109/lawp.2014.2325025.

[18] Mohammed, J.; Sayidmarie, K. Planar array with optimized perimeter elements. In Proceedings of the 1st International Multi-Disciplinary Conference Theme: Sustainable Development and Smart Planning, Antalya, Turkey, 28–30 June 2020, http://dx.doi.org/10.4108/eai.28-6-2020.2297890.

[19] Mohammed, J.R. Design of printed Yagi antenna with additional driven element for WLAN applications. *Prog. Electromagn. Res. C* **2013**, *37*, 67–81, https://doi.org/10.2528/pierc12121201.

[20] Bansal, R. Antenna theory; analysis and design. *Proc. IEEE* **1984**, *72*, 989–990, https://doi.org/10.1109/proc.1984.12959.

[21] Mohammed, J.R. A novel linear and planar multiband fractal‐shaped antenna arrays with low sidelobes. *Int. J. Commun. Syst.* **2024**, e5736, https://doi.org/10.1002/dac.5736.

[22] Hu, G.; Wu, Q.; Xu, K.; Si, J.; Al-Dhahir, N. Secure Wireless Communication via Movable-Antenna Array. *IEEE Signal Process. Lett.* **2024**, *31*, 516–520, https://doi.org/10.1109/lsp.2024.3359894.